

The GlueX Central Drift Chamber

GlueX-doc-744 (version 1)

Curtis A. Meyer
Carnegie Mellon University

February 2007

Introduction

The GlueX Central Drift Chamber (CDC) will be a 1.75 *m* long chamber that sits at the upstream end of the GlueX solenoid and surrounds the liquid hydrogen target. It will be used to track particles coming from the GlueX target with polar angles between about 6° and 155° with optimal coverage from about 20° to 140°. Tracks going more forward than about 20° will be tracked by both the CDC and the Forward Drift Chamber (FDC) systems. These tracks will need to travel through the downstream end plates of the CDC, so minimizing the material in this plates is extremely desirable.

The use of a straw-tube chamber in this region allows us to accomplish this goal as the straws can easily support the ~ 50 *g* of tension on each of the ≈ 3350 anode wires in the chamber. If one were to go with a wire-cage geometry using field wires, one would need to support about 3000 *kg* of tension between the the end plates. Something which would require both thick end plates as well as thick shell material at both the inner and outer radius of the chamber.

In addition to minimizing material, the straw-tube designs also allows for an extremely well defined electric field through which the ionization drifts. This is especially important given the 2.24 *T* magnetic field. With straw-tubes, the time-to-radius relation can be quite accurately computed using programs such as GARFIELD, and is extremely simple to implement in reconstruction. It also minimizes dead areas in the electric fields which are extremely difficult to model and lead to very poor position resolution for

tracks passing near such regions. A situation which is almost impossible to avoid with wire-cage arrangements.

In order to achieve the physics goals of GlueX, the CDC needs to be able to measure perpendicular distances from the wires ($\sigma_{r\phi}$) to an accuracy of $\approx 150 \mu m$. It also needs to be able to make some measurements along the length of the wire (σ_z) to an accuracy of about $2 mm$ and be able to make dE/dx measurements that will allow us to separate kaons and pions below $450 Mev/c$. The $\sigma_{r\phi}$ can be obtained in the straw tube arrangement. The σ_z will be achieved by placing about $\frac{1}{3}$ of the straw tubes at stereo angles of $\pm 6^\circ$ relative to the straight wires. The dE/dx will be achieved by reading out the tubes using Flash ADCs (FADCs) and then making path length corrections.

The CDC Geometry

The planned design for the CDC is shown schematically in Figure 1. The active region is $175 cm$ long with a $0.6 cm$ thick down-stream end plate and a $0.9 cm$ thick up-stream endplate. At the down-stream end is a $5 cm$ thick gas plenum which collects the gas from the tubes. At the upstream end a $10 cm$ thick plenum for distributing gas and then an additional $10 cm$ of space for electronics. All cables will be taken off the up-stream end of the chamber. The inner and outer radius of the end plates are $9 cm$ and $59 cm$ respectively.

Radially, the chamber will consist of 25 layers of straw tubes arranged in rings around the beam line. The straw tubes are $0.8 cm$ radius aluminized kapton tubes which surround a gold-plated Tungston wire. Eight of the layers are placed at stereo angles of $\pm 6^\circ$. Table 1 shows the number of straws in each layer as well as the radius of each layer. Note that for the stereo layers, the radius at the center of the chamber and that at the endplates are different. This creates an apparent dead space in the chamber volume.

In Figure 2 are shown where the holes for the straw tubes will be drilled in the upstream end plate. The straight wires are shown in black, while the stereo layers are shown in colour. The layout of the chamber and machining instructions are generated by a simple computer code that takes as input the inner and outer radius as well as which layers are stereo. It then lays out the chamber such that all tubes in a given layer are touching each other, and an exact integer number of tubes fit into a layer. The in-layer touching is crucial as the tubes are glued together for structural strength and the integer number eliminates dead spaces as one goes around the beamline.

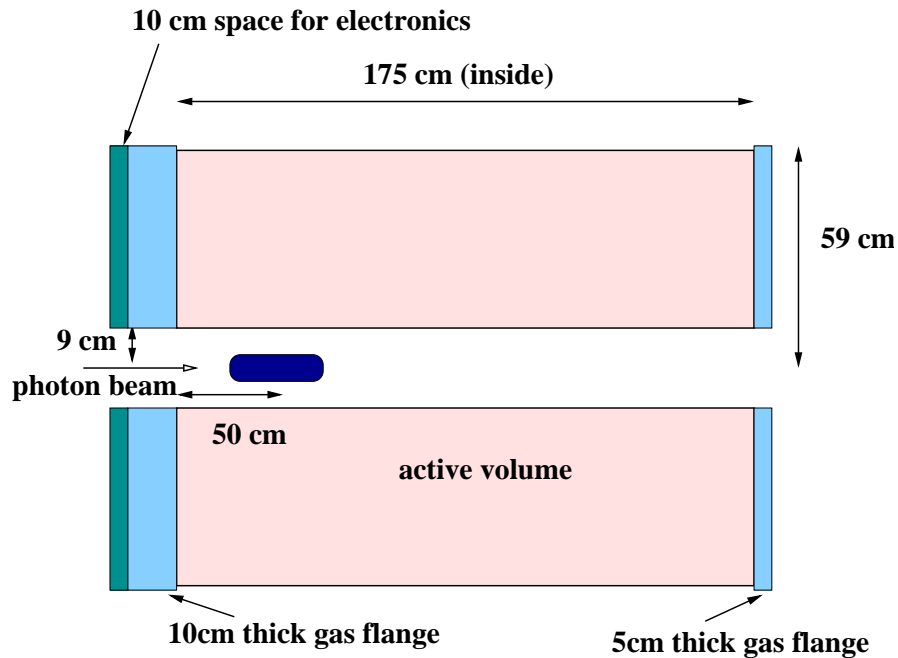


Figure 1: A side view of the CDC. The active region is 175 *cm* long with a 0.6 *cm* thick down-stream end plate and a 0.9 *cm* thick up-stream endplate. At the down-stream end is a 5 *cm* thick gas plenum which collects the gas from the tubes. At the upstream end a 10 *cm* thick plenum for distributing gas and then an additional 10 *cm* of space for electronics. All cables will be taken off the up-stream end of the chamber. The inner and outer radius of the end plates are 9 *cm* and 59 *cm* respectively.

The wires are held in place by a metallic crimp pin. The pin is inserted in a delrin holder that has holes to allow gas flow. This inturn is inserted into a two-piece donut which is glued into the enplate. For the upstream end, the donuts are made of aluminum to provide an electrical (ground) connection between the endplat and the aluminum on the straw tube. At the down-stream end, the donuts are made of Delrin to minimize the material in the chamber. Figure 3 shows schematically how the straight and stereo layers of tubes are attached to the end plates. In particular, one should note that for the stereo layers, the endplates are machined at a compound angle such that the end of the insert sits flat against the plate. This machining puts a minimum on the thickness of end plate.

| Layer | Wires | Radius (center) | Radius (plate) | Stereo |
|-------|-------|--------------------|-------------------|--------|
| 1 | 43 | 10.960 | 10.960 | |
| 2 | 50 | 12.741 | 12.741 | |
| 3 | 57 | 14.522 | 14.522 | |
| 4 | 64 | 16.304 | 18.718 | +6° |
| 5 | 71 | 18.086 | 20.289 | +6° |
| 6 | 78 | 19.868 | 21.892 | -6° |
| 7 | 85 | 21.650 | 23.522 | -6° |
| 8 | 99 | 25.214 | 25.214 | |
| 9 | 106 | 26.997 | 26.997 | |
| 10 | 113 | 28.779 | 28.779 | |
| 11 | 120 | 30.561 | 30.561 | |
| 12 | 127 | 32.344 | 32.344 | |
| 13 | 134 | 34.126 | 35.343 | +6° |
| 14 | 141 | 35.908 | 37.067 | +6° |
| 15 | 148 | 37.691 | 38.796 | -6° |
| 16 | 155 | 39.473 | 40.530 | -6° |
| 17 | 166 | 42.274 | 42.274 | |
| 18 | 173 | 44.057 | 44.057 | |
| 19 | 180 | 45.839 | 45.839 | |
| 20 | 187 | 47.621 | 47.621 | |
| 21 | 194 | 49.404 | 49.404 | |
| 22 | 201 | 51.186 | 51.186 | |
| 23 | 208 | 52.969 | 52.969 | |
| 24 | 215 | 54.751 | 54.751 | |
| 25 | 222 | 56.534 | 56.534 | |

Table 1: Shifted in Wire Layout. This has 3337 instrumented wires.

An problematic issue that is common with straw-tube chambers is the conductive glue joints that both hold the straws to the feed throughs as well as the feed throughs to the chamber end plates. Careful examination of an existing straw tube chamber from the Brookhaven EVA experiment showed that all of these joints tend to develop leaks over time. In order to try to alleviate this leak problem, a detailed study of many conducting and non-conducting epoxies was carried out to see if a good glue could be found. The conclusion of this work was that the particular choice of glue did not matter.

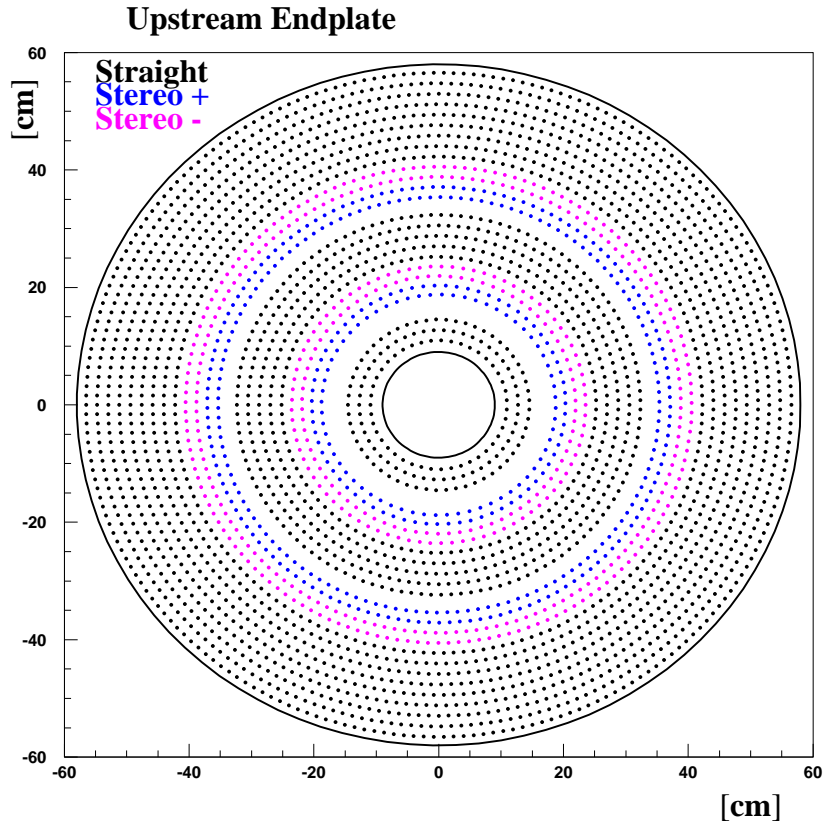


Figure 2: The drill pattern for the up-stream endplate using the 1 geometry. The black dots correspond to straight tubes. The blue dots are the $+6^\circ$ stereo layers while the magenta is the -6° stereo layers.

Instead, the act of inserting one part of a feed through into another part tended to scrape much of the epoxy off the contact surface. This led to a joint with many weak spots that over a short period of time, developed leaks.

Upon careful study of this, it was decided that the only way to guarantee a good glue connection was to develop a system in which one is certain the glue is actually making solid contact with both surfaces. The result of this is a feed through system as shown in Figure 4. The *donut* is a small tube with a small *glue trough* machined into its perimeter. From one end of the donut, a small *glue port* is drilled from the outside to the *glue trough*.

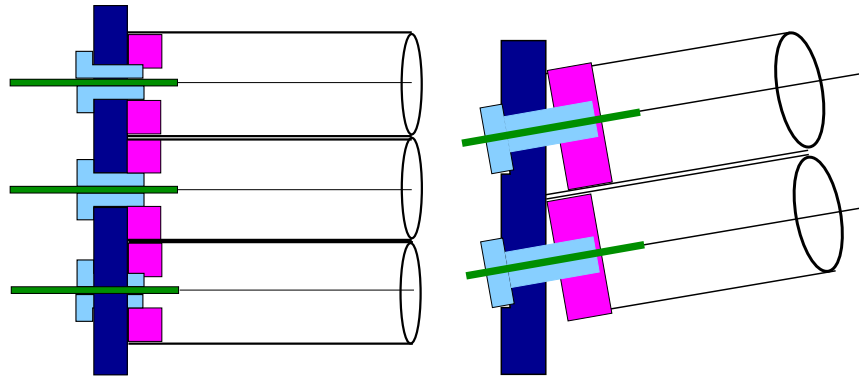


Figure 3: A schematic drawings of the feed throughs for both the normal (**left**) and stereo (**right**) wires in the CDC.

Once the donut has been inserted into the straw tube, a known amount of conducting epoxy can be injected through the *glue port* into the *glue trough*. The strength of the resulting glue joint is solid, independent of the tested epoxies. In fact several test sells have maintained several psi overpressure for nearly nine months without leaking.

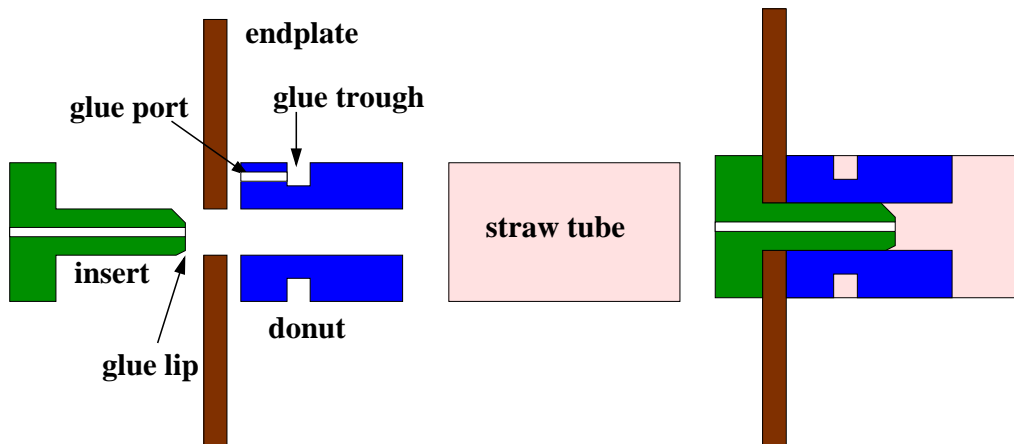


Figure 4: The CMU designed feed throughs which provide a solid glue joint between the straw-tube and the end plate. The left-hand figure shows an expanded view, while the right-hand shows the feed throughs in the chamber end plates.

Into the donut, it is necessary to glue the insert that both holds the straw

tube the chamber end plate and holds the crimp pin. In order to guarantee a good glue joint between the donut and the insert, a small *glue lip* has been machined on the tip of the insert. If a uniform coat of glue is applied to the outside of the *insert*, then when it is inserted into the donut, the epoxy tends to collect in both the *glue lip* and between the *insert* and the chamber end plate. Exactly where we need it to guarantee a good epoxy seal. Using these specially designed feed through systems, we are able to obtain a conducting gas-tight joint with all conducting epoxies that we have tried.

It is these donuts that will be machined out of aluminum for the upstream end plate and delrin for the down-stream endplate. These parts have been manufactured at Carngie Mellon university for the prototype chamber.

The straw tubes are clearly a crucial element of the design. Work has been done with both aluminized mylar and aluminized kapton tubes. It was found that the mylar tubes were not particularly forgiving during the construction process. Any kink or bump tended to remain in the tube, thus destroying its usefulness. In contrast, the kapton tubes tended to bounce back from just about anything. Once in place, they are much more resilient and significantly less prone to damage. The two main draw backs to kapton are the fact that they are somewhat more expensive than mylar, and that their *springiness* makes them more prone to gravitational sag. Gluing them securely to their neighbor tubes in the final chamber is crucial. However, based on experience with both, it has been decided that kapton tubes will lead to a more resilient chamber, and based on the significantly lower rejection rate (5% versus 95%), will ultimately cost less than mylar.

The Chamber Gas and the Gas System

The choice of chamber gas plays a significant role in the chamber's performance due to the $2.24T$ magnetic field. In order to study this, the GARFIELD program [?] has been used to compute electrostatic properties of the straw tubes, both with and without the magnetic field. The results of this work can be summarized in GlueX note 62.. Figure ?? shows an electrostatic calculation for a tube with the wire well-centered in it. Figure 5 shows GARFIELD calculations for two tracks going through a straw tube in three different gas mixtures. The three gas mixtures are Ar(30%)-C₂H₅(20%)-CO₂(50%), Ar(90%)-CO₂(10%) and Ar(50%)-C₂H₅(50%). While in all three cases the time-to-distance relationship is well defined, the longer drift distances of the spiraling tracks introduce a large diffusion contribution to the total resolution. The diffusion resolution, σ_L is also dependent on the gas. Pure argon has an extremely poor resolution, while pure carbon dioxide has a very good resolution. Finally, it is desirable to collect the electrons as quickly as possible. A slow gas, or a very long drift distance can easily push the collection time over a micro second. For this reason, the Argon-Ethane mixture shown in the lower two plots of Figure 5 is an inappropriate mixture. Investigations are ongoing to identify mixtures that will satisfy all of the requirements. To indicate the advantage of good electrostatics, Figure 6 shows what happens to the time-to-distance relation as one goes from zero magnetic field to full magnetic field.

In order to achieve the desired $150\ \mu m$ resolution in the CDC, we need to account for all possible contributions to the resolution. Table 2 summarizes these. Clearly the most important is the diffusion term, which depends on the gas. In order to achieve this, a gas mixture that contributes about $120\ \mu m$ for an average $5\ mm$ drift in a $\sim 2.5\ kV/cm$ electric field needs to be used. Many gas mixtures satisfy this requirement. The next largest contribution is the gravitational sag. This scales with the length squared, and will go down if the chamber is shorter than $1.75\ m$. The timing resolution of $45\ \mu m$ assumes that the signal is digitized using $125\ MHz$ flash ADCs and that a timing algorithm that yields times to about $\frac{1}{3}$ of the digitization are used. Time fitting algorithms that are matched to the pulse shape in chambers usually yield intrinsic time resolutions around 20% of the time bin width.

Currently work is being carried out using a 90% Argon, 10% Carbon-dioxide gas mixture. The gas system currently in use for the prototype will likely evolve into the final system. It consists of an electronic mixer that can

| Effect | Resolution μm |
|--------------------------|--------------------|
| Diffusion σ_L | 50 to 200 μm |
| Geometrical Precision | 40 μm |
| Gravitational Sag | 56 μm |
| Electrostatic Deflection | 10 μm |
| Timing Resolution | 45 μm |
| Quadrature Total | 96 to 216 μm |
| Design Resolution | 150 μm |

Table 2: The estimated contributions to the ultimate chamber resolution from various known effects. These numbers are based on 1.75 m long, 20 μm diameter, Au-W wires under 50 g tension.

handle four gas inputs with individually calibratable controls. The resulting mixture is then pushed into a mixing tank, and then delivered to the chamber. The four input gasses are filtered before entering the system. One of the gas values allows for its output to be bubbled through a chilled liquid such as water or methylal. The current design calls for several gas changes per day in the chamber with the exhaust gas being discarded. Monitors will need to be installed to monitor the temperature and the oxygen content of the input gas. In addition, a slight over-pressure system will be used to keep the gas pressure slightly above the current atmospheric pressure. Such a system will require monitoring the atmospheric pressure and ultimately correcting the chamber calibrations based on the density of the chamber gas.

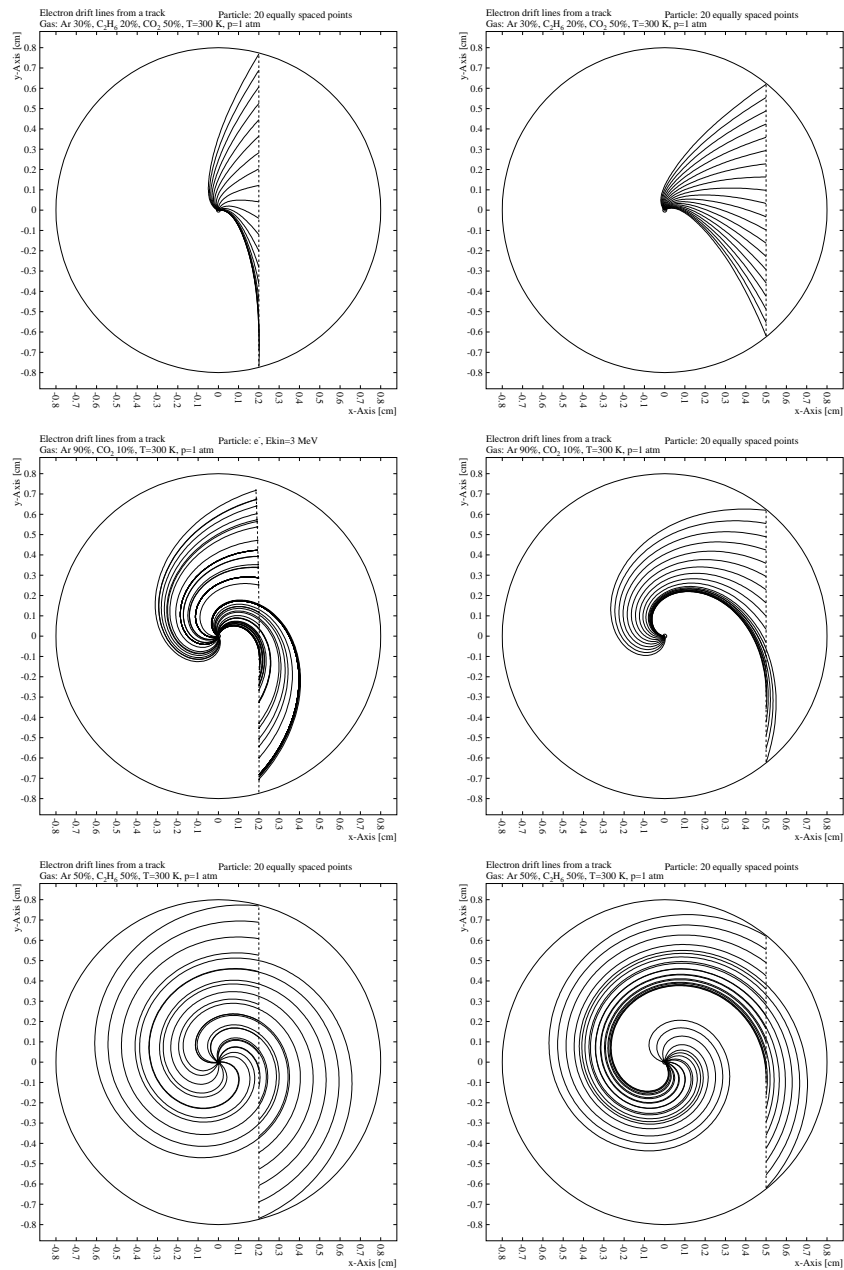


Figure 5: GARFIELD simulations of electrons drifting through a straw tube in the CDC. The curved shape of the tracks is due to the Lorentz angle induced by the 2.25 T magnetic field.

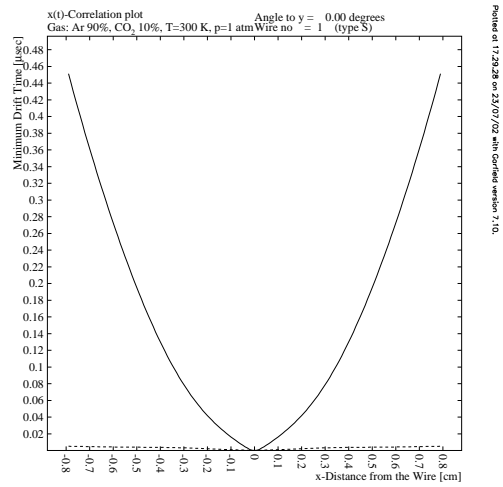
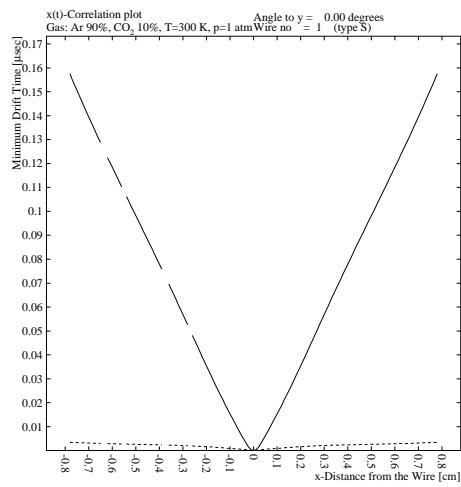


Figure 6: Calculated time versus distance in 90% Argon, 10% Carbon Dioxide mixture. **left**: No magnetic field, **right**: full magnetic field.

Chamber Electronics

Chamber Installation and Calibration

Background Rates in the Chamber

Since that time, it was realized that the magnetic field near the beam axis was not included in the original background estimates. The studies have been redone and it now looks reasonable to move the layers of the CDC closer to the beam line.

Table 1 shows a proposed placement of the the layers of the CDC. It moves the layers in such that they span from about 11 *cm* to 56 *cm* ($L = 45$ *cm*), and moves the first stereo layers into a radius of about 16 *cm*. These changes would improve both momentum and vertex resolution of the chamber as well as freeing up space between the CDC and the BCAL for infrastructure that may be needed. The one possible issue is that for the inner layer to be at about 11 *cm*, the inner radius of the end plates and shell of the chamber would need to be at about 9 *cm* radius.

List of Design Parameters

Table 3: Geometry

| | |
|---|------------------------|
| Active volume inner radius: | 10.16 <i>cm</i> |
| Active volume outer radius: | 57.4 <i>cm</i> |
| Active length: | 175 <i>cm</i> |
| Chamber assembly outer radius: | 60.0 <i>cm</i> |
| Axial layers (1-4): | 10.2 to 15.3 <i>cm</i> |
| Stereo layers (5-8): | 15.9 to 22.5 <i>cm</i> |
| Axial layers (9,13): | 24.4 to 33.2 <i>cm</i> |
| Stereo layers (14-17): | 33.4 to 40.3 <i>cm</i> |
| Axial layers (18,23): | 41.5 to 57.4 <i>cm</i> |
| Thickness per layer (g/cm ²): | 0.051 |
| Thickness per layer (rad. lengths): | 0.0014 |
| Thickness per 25 layers (rad. lengths): | 0.035 |

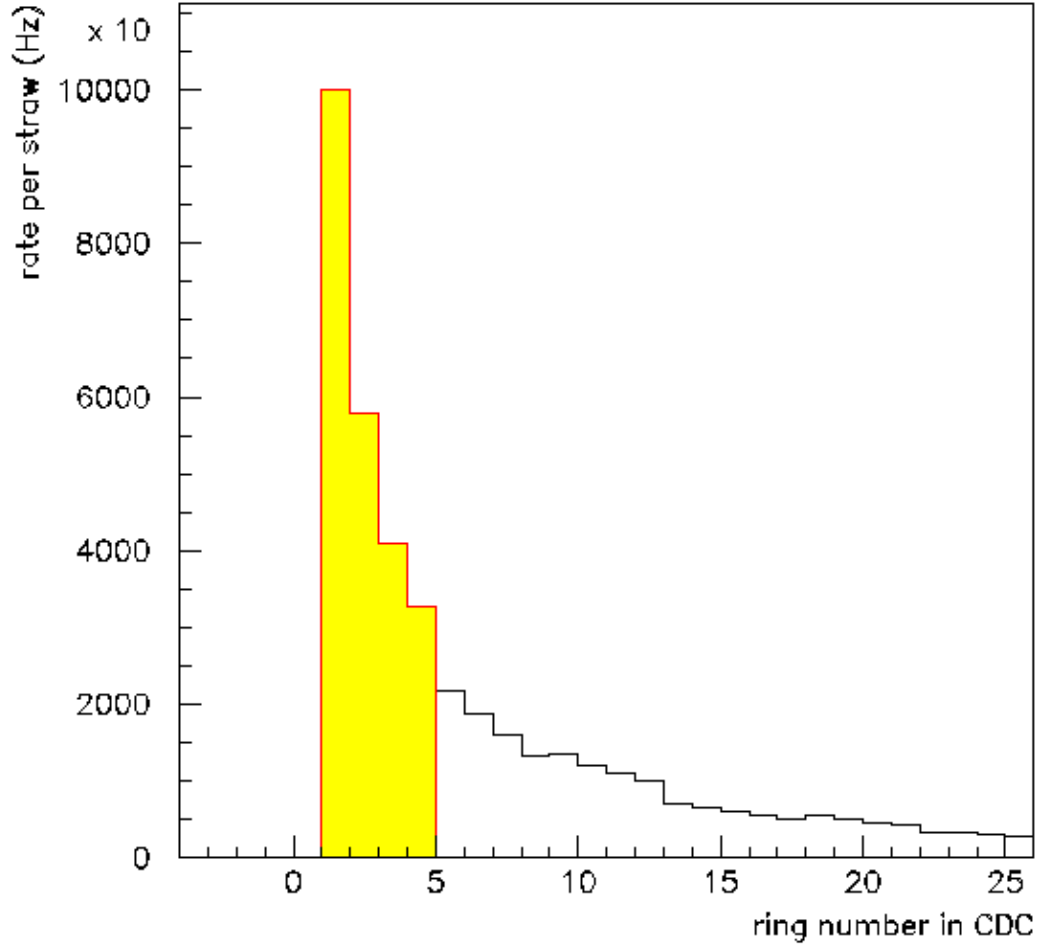


Figure 7: The electromagnetic background rates as a function of layer in the CDC for 10^8 tagged photons per second. The rates are per tube with the innermost four tubes placed at 6.12 cm , 8.15 cm , 10.19 cm and 12.02 cm respectively. Even at a 6 cm from the target, the background rate is only 100 KHz .

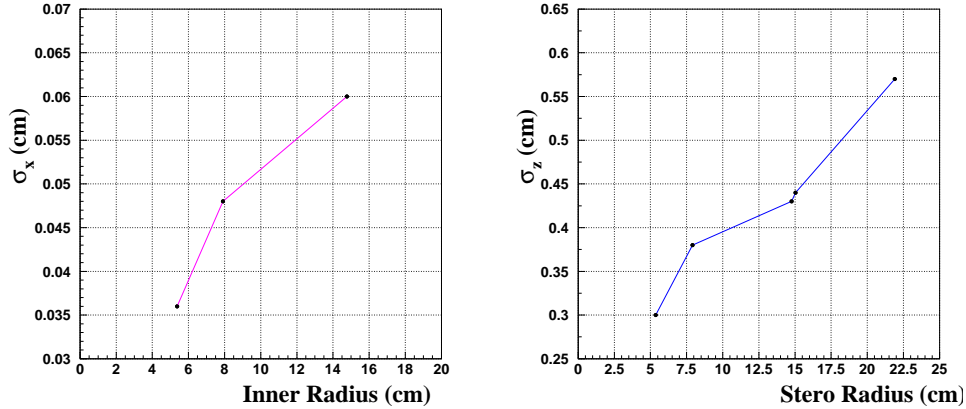


Figure 8: The estimated vertex resolution as a function of the radius of the innermost layer of tubes. For the case of the x resolution, this corresponds to the straight layers. For the z resolution, it is a function of the location of the first stereo layer.

Response to the GlueX Detector Review

The original CDC design had an active length of 200 cm and 23 instrumented layers going from about 16 cm to 58 cm radius ($L = 42$ cm). The wire layout is summarized in Table 10. As indicated in the table, the smallest radius of a stereo wire is about 23 cm at the center of the chamber.

One of the questions raised at the GlueX detector review had to do with vertex resolution and the placement of the stereo layers. It was suggested that the stereo layers be brought closer to the beam line to improve the z -vertex resolution from tracks. A careful study was carried out on this shortly after the review and concurred that moving both the straight and stereo layers closer to the beam axis would make a significant improvement in vertex resolution. Unfortunately, background estimates at the time indicated that moving closer to the beam line was not an option.

Table 4: Material

| | |
|---|---------------------------------------|
| Gas (at 1 at.): | $Ar/CO_2/CH_4$ 80/10/10 (possibly) |
| Number of cables : (50-conductor shielded ribbon cables) | 3337/24 |
| Positioning accuracy of sense wires (x,y): | 10 μm |
| Positioning accuracy of package (z): | 0.5 mm |
| Thickness of inner shell (g/cm ²): | 0.162 |
| Thickness of inner shell (rad. lengths): | 0.0067 |
| Thickness of outer shell (g/cm ²): | 1.02 cm of fiberglass |
| Thickness of outer shell (rad. lengths): | 0.031 |
| Strawtube (diameter): | 1.6 cm |
| Strawtube (material): | Aluminized Kapton |
| Strawtube (thickness): | 100(5) μm Kapton(Al) |
| Number of sense wires (20 micron gold-plated W): | $3337 \pm 1.5\%$ |
| Upstream Endplate: | 0.9 cm Al |
| Downstream Endplate: | 0.6 cm Al |
| Upstream Feedthrus: | Al |
| Downstream Feedthrus: | Delrin |
| Plenums: | Plexiglas |

Table 5: Location active area

| | |
|---------------------------|--------|
| Upstream gas plenum: | -3 cm |
| Upstream active volume: | 17 cm |
| Downstream active volume: | 192 cm |
| Downstream gas plenum: | 202 cm |

Table 6: dE/dX capability

| | |
|-----------------|--------------------|
| Sense wires: | YES |
| Momentum Range: | $p \leq 450 MeV/c$ |

Table 7: Operation:

| | |
|------------------------------------|-----------------|
| Nominal operating voltage (sense): | +1900 V |
| Nominal gas gain: | 5×10^4 |
| Gas flow: | 5/day |

Table 8: Preamplifier and Readout

| | |
|---------------------------|-------------------------|
| Nominal gain: | 5^4 |
| Noise level: | |
| Rise time: | $\sim 50 \text{ ns}$ |
| Tail compensation: | YES |
| Cable length to post-amp: | 30 m |
| Discriminator output: | NO |
| Sense wires: | 100 MHz FADCs |

Table 9: Calibration and Resolution

| | |
|--------------------------------------|-------------------|
| Sense wires (selected charge): | electronic pulser |
| Perpendicular to wire (σ): | $150 \mu\text{m}$ |
| z-position from stereo (σ): | 2 mm |
| z-position from charge division: | 8 cm |

Table 10: Reference Wire Layout. This has 3349 instrumented wires.

| Layer | Wires | Radius (center) | Radius (plate) | Stereo |
|-------|-------|--------------------|-------------------|--------|
| 1 | 63 | 16.049 | 16.049 | |
| 2 | 70 | 17.831 | 17.831 | |
| 3 | 77 | 19.613 | 19.613 | |
| 4 | 84 | 21.395 | 21.395 | |
| 5 | 91 | 23.178 | 25.449 | +6° |
| 6 | 98 | 24.960 | 27.082 | +6° |
| 7 | 105 | 26.742 | 28.733 | -6° |
| 8 | 112 | 28.524 | 30.398 | -6° |
| 9 | 126 | 32.089 | 32.089 | |
| 10 | 133 | 33.871 | 33.871 | |
| 11 | 140 | 35.654 | 35.654 | |
| 12 | 147 | 37.436 | 37.436 | |
| 13 | 154 | 39.218 | 39.218 | |
| 14 | 161 | 41.001 | 42.326 | +6° |
| 15 | 168 | 42.783 | 44.055 | +6° |
| 16 | 175 | 44.566 | 45.788 | -6° |
| 17 | 182 | 46.348 | 47.525 | -6° |
| 18 | 193 | 49.149 | 49.149 | |
| 19 | 200 | 50.932 | 50.932 | |
| 20 | 207 | 52.714 | 52.714 | |
| 21 | 214 | 54.497 | 54.497 | |
| 22 | 221 | 56.279 | 56.279 | |
| 23 | 228 | 58.062 | 58.062 | |